NEAR-WALL INFLUENCE OF LARGE-SCALE MOTIONS IN HIGH REYNOLDS NUMBER TURBULENT BOUNDARY LAYERS

B. Ganapathisubramani
Department of Aeronautics, Imperial College London.
g.bharath@imperial.ac.uk

N. Hutchins, J. P. Monty, H. Ng, & I. Marusic
Department of Mechanical and Manufacturing Engineering,
University of Melbourne, Australia

ABSTRACT

A spanwise array of surface hot-film shear-stress sensors and a traversing hot-wire located directly above one of these sensors are used to examine the relationship between skin-friction fluctuations and the velocity fluctuations in the boundary layer. Experiments are performed in a high Reynolds number turbulent boundary layer at $Re_\theta \approx 39000$. The shear-stress data indicate the presence of large-scale structures that extend to large streamwise distances. These structures appear to be the footprint of the large-scale superstructures that are present in the logarithmic region. Conditional averages computed based on low and high skin-friction events indicate the presence of a forward-leaning low-speed and high-speed structure, respectively. The velocity fluctuations from the hot-wire are decomposed in to large-scale and small-scale components respectively. The decomposed signals are used to compute conditionally-averaged turbulence intensities conditioned on low and high skin-friction events. The results show that the low-speed structure associated with the low skin-friction event consists of weak small-scale fluctuations near the wall and intense small-scale fluctuations farther away from the wall. Conversely, the high-speed structure associated with high skin-friction event possesses intense and weak small-scale activity near and farther away from the wall, respectively.

INTRODUCTION

Wall-bounded turbulent flows are composed of recurring features (called 'coherent structures'). The scope and description of these features has evolved over several decades from hairpin vortex to vortex clusters. However, a recurring pattern that is consistent with all these coherent structures is the presence of elongated narrow strips of uniform momentum. The presence of these elongated low- and high-speed regions in the logarithmic region of wall-bounded turbulent flows is well documented (Tomkins & Adrian, 2003; Ganapathisubramani et al. 2003; Hutchins & Marusic 2007a among others). Hutchins & Marusic (2007a) found that these low- and high-speed regions meander in the spanwise direction and cover a much larger streamwise domain than previously identified. They termed these elongated meandering large-scale motions as 'superstructures'. These motions play an important role in the dynamics as they carry a significant amount of Reynolds shear stress (Guala et al., 2006).

Bandyopadhyay & Hussain (1984) studied the relationship between large-scale and small-scale motions and found a significant coupling between the scales over a range of flows (jets, wakes and boundary layers). Hutchins & Maru-

sic (2007b) examined the interaction between the large-scale and small-scale motions in the near-wall region by decomposing hot-wire signals obtained at $y^+ = 15$ in a high Reynolds number turbulent boundary layer (where, y is the wall-normal direction, and the superscript $+$ denotes normalisation using skin friction velocity, U_τ, and kinematic viscosity, ν). They found that the large-scale motions appeared to modulate the small-scale component of the velocity fluctuations. Recently, Mathis et al. (2009) have found that the extent of modulation depends on the Reynolds number.

Given that the large-scale motions have a substantial impact on a variety of flow properties, it is natural to explore their involvement in the near-wall cycle and their contributions to the skin friction drag. In fact, Abe et al. (2004) concluded that very large structures exist in the outer layer, and that these structures are instantaneously visible in the surface shear-stress fluctuations. In this study, we aim to explore the relationship between the large-scale coherence in skin friction fluctuations and the velocity fluctuations in the boundary layer. The objective, is to perform simultaneous velocity and surface shear stress measurements (similar to those performed by Brown & Thomas, 1977; Wark & Nagib, 1991 among others) to examine the relationship between velocity fluctuations in the outer region of a boundary layer and the shear stress at the wall.

EXPERIMENTS

Experiments are performed in purpose-built high Reynolds number turbulent boundary layer facility at the University of Melbourne. The tunnel is an open return blower wind tunnel with a 27 m working length and a 2×1m cross-section. Measurements are carried out 21 m downstream of the trip on boundary layers developing on the tunnel floor. Measurements are performed at a free-stream velocity of 20 m/s. The 99% boundary layer thickness (δ) at the measurement location is 0.26 m, the displacement thickness is 0.036 m, the momentum thickness (θ) is 0.029 m, the skin friction velocity (obtained through a Clauser fit) is 0.665 m/s. Based on these values, the Reynolds number based on momentum thickness, $Re_\theta = U_\infty \theta / \nu \approx 39000$ and the Kárman number, $Re_\tau = \delta U_\tau / \nu \approx 11500$. In this paper, (U, u), (V, v) and (W, w) are the mean and fluctuating velocity components along the streamwise (x), wall-normal (y) and spanwise (z) directions, respectively.

A series of *Dantec* 55R47 hot-film shear stress glue-on sensors are used to identify the near-wall footprint of large-scale motions. These probes are glued on the tunnel floor as shown in figure 1. The spacing between adjacent probes is
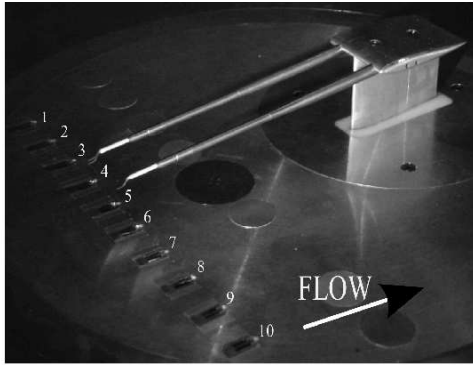
Figure 1: A perspective view of the experimental setup. The ten surface glue-on probes are numbered. They are separated by 26 mm. The two hot-wires are mounted on a sting that is traversed in the wall-normal direction.
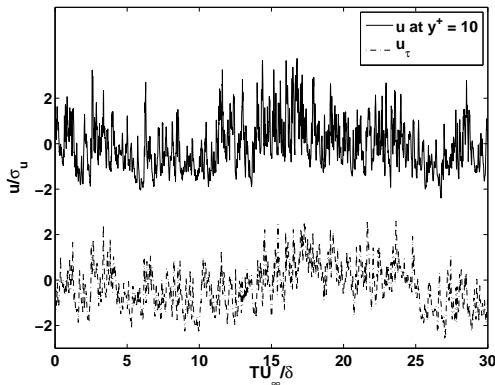

Figure 2: Time series of skin friction fluctuations and velocity fluctuations at $y^+ = 10$. The data was obtained simultaneously at the same acquisition rate with the hot-wire located directly above the glue-on probe.

nominally 26 mm (this corresponds to approximately 0.1δ). Simultaneous measurements of velocity fluctuations are performed using hot-wire anemometry. Two hot-wires are used for these measurements and they are located atop probes 5 and 6 as shown in figure 1. Wall-normal profiles of streamwise velocities are obtained by traversing the wires in the wall-normal direction. The results presented in this paper only utilises the velocity data obtained by the hot-wire on top of probe 5. This hot-wire is a Dantec 55P05 (prong spacing 3 mm) with sensor length $l = 1$ mm ($l^+ = 44$), wire diameter $d = 5\mu$m and is operated in constant temperature mode using AA labs AN1003 anemometers with overheat ratio 1.8.

For calibration, the traversing hot-wire probe is positioned in the freestream and statically calibrated *in-situ* against a Pitot-static tube pair before and after each boundary layer traverse. Third-order polynomial curves are fitted to the calibration data. Atmospheric conditions are monitored continuously throughout the experiments using a calibrated thermocouple and an electronic barometer. Linear interpolation between the pre- and post-calibration curves is used to correct for temperature change during the course of the experiment. During the same calibration process, the 10 wall-mounted glue-on sensors are also simultaneously sam-
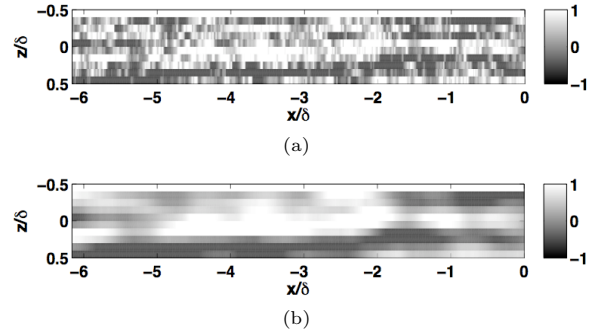

Figure 3: Iso-contours of (a) raw skin-friction fluctuations and (b) filtered skin-friction fluctuations. The fluctuations are normalised by their standard deviations (σ_{u_τ}). The streamwise extent is reconstructed by using Taylor's hypothesis assuming a convection velocity of $0.8U_\infty$.

pled, such that calibration curves are obtained for the output of each hot-film sensor as a function of U_∞. Using existing data obtained in the same facility (Mathis *et al.*, 2009), it is possible to obtain an approximate expression for friction velocity U_τ as a function of Re_x ($U_\infty x/\nu$). This empirical expression has the approximate form,

$$U_\tau = U_\infty/(C_1 + C_2 \log Re_x), \qquad (1)$$

which assumes that U_∞/U_τ varies log-linearly with Reynolds number. A best fit to this formula suggests $C_1 \approx -1.23$ and $C_2 \approx 1.86$. It should be noted that there is considerable uncertainty in this approximation. For the experimental data used in formulating equation (1), U_τ is obtained using the Clauser technique (based on the constants $\kappa = 0.41$ and $A = 5.0$).

A comparison between the velocity fluctuation at $y^+ = 10$ and the skin friction fluctuation obtained from the probe 5 (that is located directly beneath the hot-wire) is shown in figure 2. The time traces clearly reveal a remarkable similarity in the low-frequency content of the two signals. The small-scale activity in the shear stress signal appears to be attenuated. This is expected as the frequency information that can be gathered from these hot-films is limited. In the current study, the aim is to explore the influence of large-scale events in the near-wall region and noting the remarkable similarity in the low-frequency content of the hot-film and hot-wire signal, the shear-stress data is deemed suitable for further analyses. It must also be noted that the uncertainty in the shear-stress information also stems from the calibration process. For example, the Clauser technique with altered constants (κ and A) will yield different estimates of U_τ. However, these uncertainties have minimal effect on the analysis presented in this paper as the spanwise array is used simply to detect the passage of large-scale high and low skin-friction events.

SKIN-FRICTION FLUCTUATIONS

The skin friction fluctuations from the spanwise array of probes can be used together with Taylor's hypothesis to decipher a pseudo spatial length scale of the large-scale structures. Assuming frozen field convection, a streamwise-spanwise distribution of the skin friction fluctuations is reconstructed by using a convection velocity of $0.8U_\infty$. Figure 3(a) shows skin friction iso-contours at the wall. It must be noted that streamwise extent is based on an arbitrary
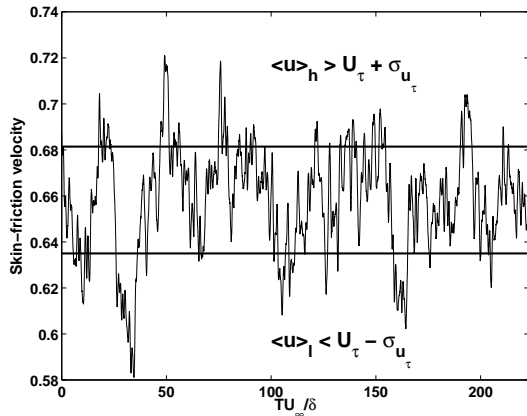
Figure 4: Filtered skin-friction velocity from probe 5. The horizontal solid lines show the thresholds used to detect the high and low skin-friction event for conditional analysis.

convection velocity ($0.8U_\infty$) and further work is required to determine the convection velocity of the structures at the wall. Regardless, the plot shows the presence of meandering elongated low- and high shear-stress regions. However, these elongated regions also contain smaller scale fluctuations within them. Since the small scale skin-friction fluctuations are not necessarily reliable as the frequency response of the surface probes is limited, the data is smoothed by using a Gaussian filter of size approximately $0.5\delta \times 0.1\delta$ (streamwise $\times$ spanwise) to remove the effects of the small-scales. Figure 3(b) depicts the streamwise-spanwise distribution of the filtered skin-friction fluctuations that clearly reveals the presence of an elongated large-scale low skin-friction region (in black) located adjacent to an elongated high skin-friction region (in white). Such elongated regions of uniform low- and high-speed regions were observed by various other studies in the logarithmic region of wall-bounded turbulent flows over a range of Reynolds and Mach numbers (Hutchins & Marusic, 2007a; Ganapathisubramani *et al.*, 2006; Monty *et al.*, 2007). This suggests that the elongated low and high skin-friction regions at the wall could be related to the large-scale superstructures in the logarithmic region. This is in stark contrast to the consensus view in the literature that there is a separation between the near-wall structure and the log-region/outer structures.

CONDITIONAL EVENTS

The relationship between the large-scale skin-friction fluctuations and the velocity fluctuations in the boundary layer that may be responsible for the skin-friction fluctuations can be examined by computing conditional quantities from the hot-wire probe conditioned on the presence of low/high skin-friction event. The low skin-friction event is one where the instantaneous skin friction fluctuation is less than one standard deviation of the filtered skin-friction signal and conversely the high skin-friction event is when the fluctuation is greater than one standard deviation. Figure 4 shows a time series of the filtered skin-friction fluctuation and the thresholds used to distinguish between low and high skin-friction events. The conditional quantities are represented with angled brackets ($<>$) and the subscripts l and h denote the low and high skin-friction conditions, respectively.
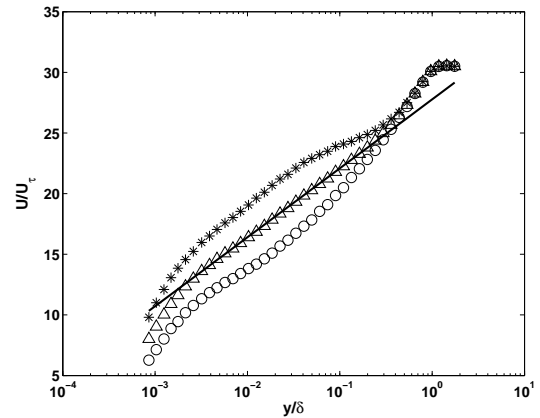

Figure 5: Wall-normal profile of average streamwise velocity. The symbols show, ($\triangle$): unconditional, U; (*): conditioned on high skin friction event, $U^+ + <u^+>_h$; ($\circ$): conditioned on low skin-friction event, $U^+ + <u^+>_l$. The solid line is the logarithmic law of the wall with $\kappa = 0.41$ and $A = 5$. The velocity is measured by the hot-wire that is located directly above glue-on probe 5.
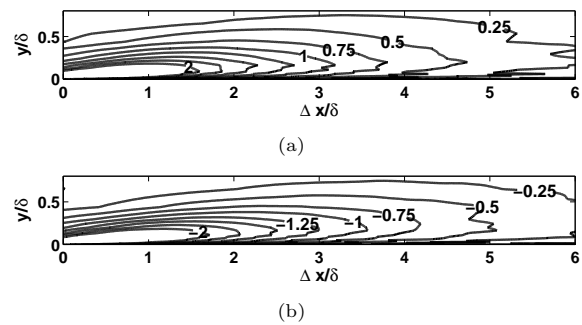

(a)

(b)

Figure 6: Iso contours of conditionally-averaged streamwise-velocity fluctuations n the streamwise-wall-normal plane. (a) Conditioned on high skin-friction event, $<u^+>_h$ and (b) Conditioned on low skin-friction event, $<u^+>_l$. The streamwise extent is computing by using Taylor's hypothesis, $\Delta x(y) = U(y)\Delta t$, where U is the unconditional mean streamwise velocity.

Conditional mean

Figure 5 shows the unconditional mean velocity profile (and the logarithmic law of the wall) together with the conditionally averaged velocity profiles. It is clear from this figure that a low skin-friction event is associated with a velocity profile that is consistently lower than the unconditional mean in the near wall and the logarithmic regions. Similarly, high skin-friction event has a velocity profile that is higher than the mean. The two conditional profiles collapse on the unconditional profile beyond $y/\delta \approx 0.5$ suggesting that the skin friction events are not influenced (and do not influence) the outer wake region of the boundary layer.

The simultaneous acquisition of skin-friction and hot-wire time-series allow us to compute conditionally-averaged velocity profiles that occur before or after a high or low skin-friction event. This time separation can be projected as a streamwise displacement using Taylor's hypothesis. Figures 6(a) and 6(b) show the streamwise-wall-normal distribution of $<u>_h$ and $<u>_l$, respectively, where the condition is the presence of a high/low skin-friction event at $\Delta x = 0$.

Sixth International Symposium on Turbulence and Shear Flow Phenomena
Seoul, Korea, 22-24 June 2009

(a)   (b)

Figure 8: Pre-multiplied energy spectrum of the streamwise velocity fluctuation at $y/\delta = 0.035$.
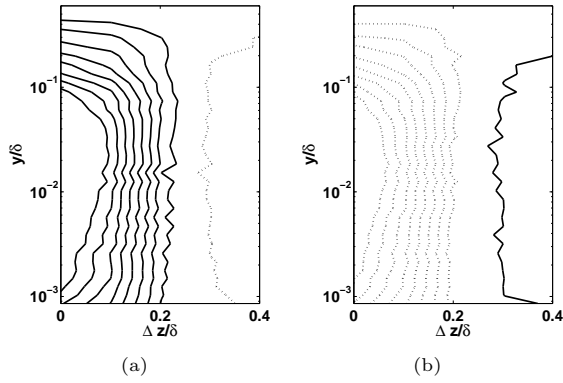
Figure 7: Contours of conditionally-averaged streamwise-velocity fluctuations in the spanwise-wall-normal plane at $\Delta x = 0$. (a) Conditioned on high skin-friction event, $< u^+ >_h$ and (b) Conditioned on low skin-friction event, $< u^+ >_l$. Contours from -2 to 2 are shown with spacing of 0.25. The zero contour is not shown. Note that the wall-normal axis is depicted in Log scale.

The contours reveal a forward-leaning high-speed structure for $< u >_h$ and a similar forward-leaning low-speed structure for $< u >_l$. It must be noted that the conditionally-averaged velocity profiles in figure 5 were extracted along a vertical line at $\Delta x = 0$. The observed forward leaning structure is consistent with Brown & Thomas (1977) and various other studies that were based on multi-hot-wire correlation measurements.

Although the hot-wire probe is located above probe 5, probes 1–4 and 6–10 together with the hot-wire signal can be used to calculate the spanwise-wall-normal signature of the conditionally-averaged structure. Figure 7(a) and 7(b) show contours of conditionally-averaged streamwise velocity fluctuation based on a high and low skin-friction event occuring at $\Delta z = 0$ and $\Delta x = 0$ (The plots show the contours only for positive z as the contours are symmetric about the y axis). Figure 7(a) shows that the structure of the high-velocity region above a high skin-friction event is located adjacent to a low-velocity region. The width of the high-speed region is approximately 0.3δ. Conversely, the low-speed region above a low skin-friction event (shown in figure 7b) is adjacent to a high-speed region. This is consistent with previous observation that elongated low- and high-speed (or skin-friction regions) are adjacent to each other in the spanwise direction. Although the spanwise and wall-normal components of the velocities are not measured in this study, results from DNS data (see Hutchins & Marusic, 2007b) suggests that these adjacent low- and high-speed regions are associated with a pair of counter-rotating roll modes. These roll modes sweep high-speed fluid to the wall and eject low-speed fluid away from the wall.

Conditional variance

It must be noted that the conditional average of the velocity consists of fluctuations across all scales. Therefore, the contributions of the large-scale velocity fluctuations (such as superstructures) cannot be differentiated from the small-scale fluctuations (near-wall streaks). Therefore, a novel method is proposed to analyse the contributions of various scales. This method was first used by Hutchins & Marusic (2007b) to explore the modulation of near-wall fluctuations by the superstructures.
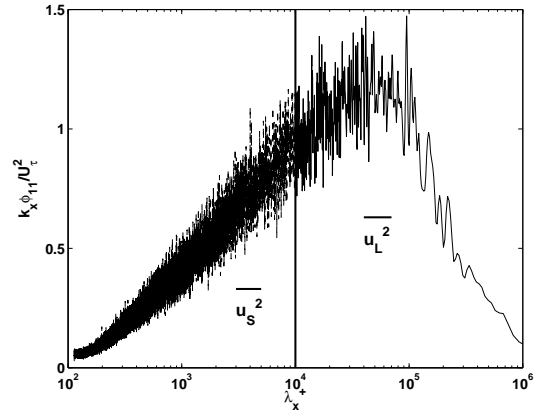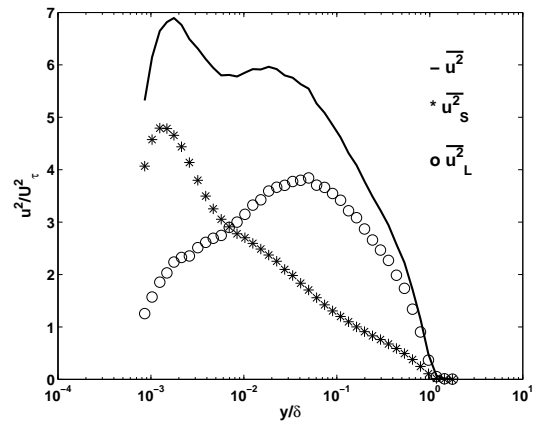

Figure 9: Streamwise turbulence intensity. Solid shows the total turbulence intensity, (*) symbols show the small-scale contribution ($\overline{u_S^2}$) and the (○) symbols show the contribution from large-scales ($\overline{u_L^2}$).

In this method, the fluctuating signals across the boundary layer are decomposed into large- and small-scale fluctuations, using a spectral filter. That is, the fourier coefficients greater than or less than $\lambda_x = \delta$ ($\lambda_x^+ \approx 10000$) are used to obtain the large-scale and small-scale decomposed signals, respectively. Consider the pre-multiplied energy spectrum depicted in figure 8 at $y/\delta = 0.035$. Also shown in the figure is a vertical line that corresponds to the spectral filter. The energy content to the left of this line (i.e., $\lambda_x^+ < 10000$) is attributed to small-scale fluctuations and the turbulence intensity computed from that area is labelled u_S^2. The energy content for $\lambda_x^+ > 10000$ are contributions from the large-scale structures and the turbulence intensity from this area is labelled u_L^2. Figure 9 shows the wall-normal profile of the large-scale and small-scale components of the streamwise turbulence intensity. The small-scale component (* symbols) accounts for the majority of the near-wall peak and decays throughout the logarithmic region. The large-scale component makes a significantly lower contribution (compared to small-scale) in the near-wall region. Having said that, it should be noted that large-scales do make a contribution turbulent fluctuations near the wall suggesting reinforcing the fact large-scale structures maintain a footprint in the near-wall region. Farther away from the wall,
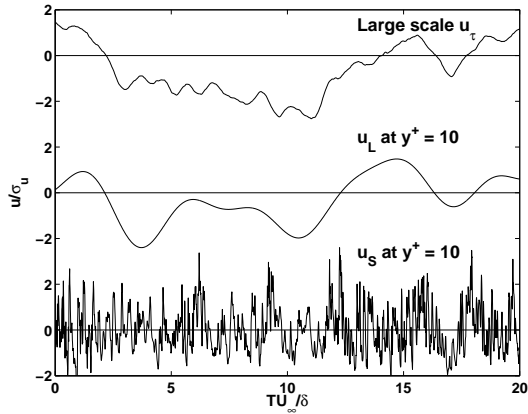
Figure 10: Comparison between the large-scale skin-friction fluctuations and the large-scale and small-scale fluctuations at $y^+ = 10$.
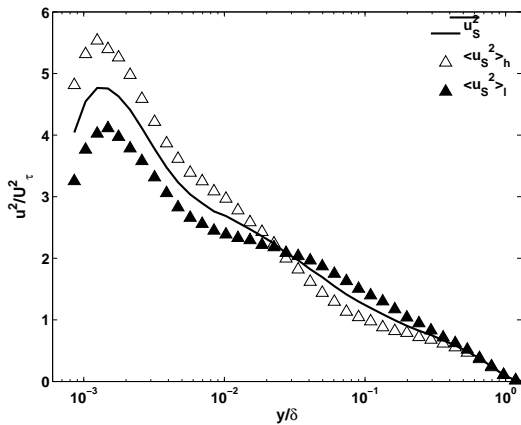

Figure 11: Wall-normal profiles of small-scale turbulence intensities conditioned on high (hollow symbols) and low (filled symbols) skin-friction events. The solid line shows the unconditional small-scale turbulence intensity.

the large-scale make an increasingly larger contribution to the turbulent fluctuations.

Figure 10 shows a comparison between the large-scale skin-friction fluctuations and the large- and small-scale velocity fluctuations at $y^+ = 10$. The figure shows that the skin-friction fluctuations are similar to the large-scale velocity fluctuations. In addition, the figure indicates that the amplitude of the small-scale fluctuations depends on the sign of the large-scale fluctuations. For negative values of large-scale fluctuations, the amplitude of small-scale fluctuations appears diminished. On the contrary, the amplitude of small-scales is higher for positive fluctuations of the large-scales. This suggests that an elongated low-speed superstructure tends to weaken the fluctuations in the near-wall streaks while a high-speed superstructure strengthens the near-wall fluctuations. This is consistent with observations made by Hutchins & Marusic (2007b) and Mathis *et al.* (2009) based on a similar analysis.

The time series of the large-scale and small-scale fluctuations (such as those shown in figure 10) can be used to evaluate the contribution of these scales to the conditional structure. A conditional mean-squared of the large-scale and small-scale fluctuations, conditioned on the occurrence of the
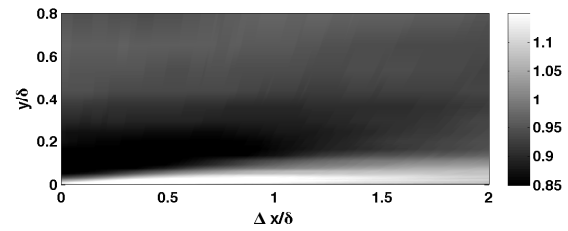
(a)
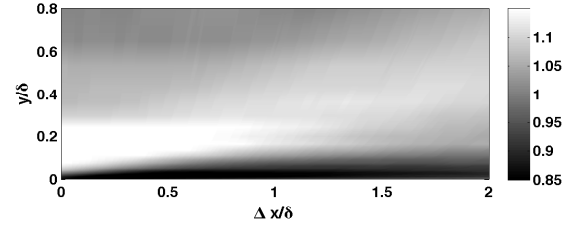
(b)

Figure 12: Contours of conditional small-scale turbulence intensity in the streamwise-wall-normal plane. The skin-friction condition is enforced at $y = 0$ and $\Delta x = 0$. (*a*) High skin-friction condition, $< u_S^2 >_h / \overline{u_S^2}$ and (*b*) Low skin-friction condition, $< u_S^2 >_l / \overline{u_S^2}$. The intensity at each wall-normal location is normalised by the local unconditional small-scale turbulence intensity.

low and high skin-friction event can be computed to evaluate the energetic turbulent structure associated with high and low skin-friction regions. Figure 11 shows wall-normal profiles of small-scale turbulence intensities conditioned on high-(hollow symbols) and low-(filled symbols) skin-friction events. Near the wall, the small-scale fluctuations conditioned on a high skin-friction event possess higher intensity than the small-scale fluctuations associated with low skin-friction events. This suggests that the near-wall small-scale fluctuations are strengthened in the presence of a large-scale high-speed event (and associated large-scale high skin-friction event at the wall).

Figure 11 shows that the intensity of $< u_S^2 >_l$ becomes higher than $< u_S^2 >_h$ at $y/\delta \approx 0.03$ ($y^+ \approx 300$) and remains higher throughout the outer log region. This indicates that the presence of a high skin-friction event near the wall leads to diminished small-scale turbulence activity away from the wall. Conversely, a low skin-friction event near the wall is associated with intense small-scale fluctuations away from the wall. This feature can be further explored by examining the streamwise-wall-normal $(x - y)$ iso-contours of conditional small-scale turbulence intensities. Figures 12(a) and 12(b) shows contours of small-scale turbulence intensity in the streamwise-wall-normal plane conditioned on high and low skin-friction events, respectively. The figures clearly reveal a forward-leaning structure in which the small-scale turbulence intensity is high near the wall and lower farther away from the wall for $< u_S^2 >_h$ and vice-versa for $< u_S^2 >_l$. The forward-leaning structure is similar to that in the structure observed in the conditional mean.

The availability of the spanwise array of probes allows us to calculate the spanwise-wall-normal distribution of the conditional small-scale turbulence intensity. Figures 13(a) and 13(b) shows iso-contours of small-scale turbulence intensity in the spanwise-wall-normal plane conditioned on high
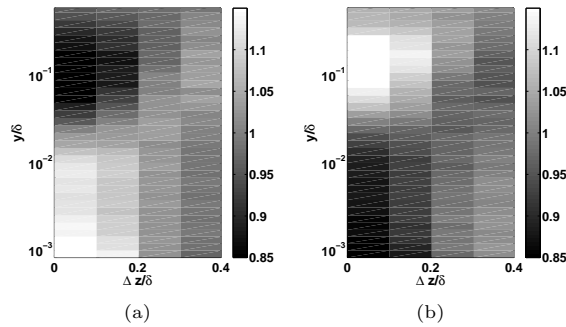
Figure 13: Contours of conditional small-scale turbulence intensity in a spanwise-wall-normal plane at $\Delta x = 0$. The skin-friction condition is enforced at $\Delta z = 0$ and $y = 0$. (a) High skin-friction event $<u_S^2>_h / \overline{u_S^2}$ and (b) Conditioned on low skin-friction event, $<u_S^2>_l / \overline{u_S^2}$. The intensity at each wall-normal location is normalised by the local unconditional small-scale turbulence intensity. Note that the wall-normal axis is in Log scale.

and low skin-friction events, respectively. The spanwise-wall-normal plane is located at $\Delta x = 0$. (Note that the conditional intensities along $\Delta z = 0$ is depicted in figure 11). Near the wall, the small-scale turbulence intensity is high for a high skin friction condition. This region is adjacent to an area of low small-scale turbulence intensity that is located at a spanwise distance of approximately $\Delta z \approx 0.3\delta$. This low turbulence intensity region is associated with a low skin-friction region. Farther away from the wall, there is depletion of turbulence intensity above the high skin-friction event at approximately $y/\delta \approx 0.02$ and this area is adjacent to a region of higher turbulence intensity. The small-scale turbulence intensity conditioned on low skin-friction event (shown in figure 13(b)) displays the opposite trends.

CONCLUSIONS

A series of glue-on probes together with a traversing hot-wire are used to identify the relationship between large-scale skin-friction fluctuations and velocity fluctuations in the boundary layer in a high Reynolds number turbulent boundary layer. The time-series from the surface glue-on probes indicate the presence of large-scale structures that extend to large streamwise distances (over 6δ in length based on Taylor's hypothesis). These structures appear to be the footprint of the large-scale superstructures that are present in the logarithmic region. A range of conditional mean and conditional variance analyses are performed to further understand the relationship between the large-scale skin friction events and the velocity fluctuations in the boundary layer. The conditional mean results indicate the presence of a forward-leaning low-speed and high-speed structure above a low and high skin-friction events, respectively. The conditional variance results show that the low-speed structure associated with the low skin-friction event consists of weak small-scale fluctuations near the wall and intense small-scale fluctuations farther away from the wall. This is consistent with the observations of Tanahashi *et al.* (2004) who observed that the fine-scale eddies in the log region is agglomerated in low-speed regions. Conversely, the high-speed structure associated with high skin-friction event possesses intense small-scale activity near the wall, switching to weaker small-scale activity beyond $y^+ > 300$.

In conclusion, this paper shows that large-scale events in the outer region of a turbulent boundary layer maintain a footprint in the near-wall region. The elongated low-/high-speed structures that are associated with low/high skin-friction events, respectively, tend to weaken/strengthen the small-scale activity near the wall in high Reynolds number turbulent boundary layers (where small scales are defined as all scales that are smaller than δ). This indicates that small-scale structures near the wall including near-wall streaks/vortices are influenced by the outer layer large-scale structures. Therefore, any control strategy for high Reynolds number wall-bounded turbulence that aims to control the small-scale activity in the near-wall region (streamwise streaks/vortices) must account for the behaviour of the large-scale structures that are present in the outer layer.

REFERENCES

Abe, H., Kawamura, H. & Choi, H., 2004, "Very large-scale structures and their effects on the wall shear-stress fluctuations in a turbulent channel flow up to $Re_\tau \approx 640$." *J. Fluids Eng.*, Vol 126, pp. 835–843.

Bandyopadhyay, P. R., & Hussain, A. K. M. F., 1984, "The coupling between scales in shear flows." *Phys. Fluids*, Vol 27(9), pp.2221–2228.

Brown G. L. & Thomas, A. S. W., 1977, "Large structure in a turbulent boundary layer." *Phys. Fluids*, Vol 20(10), pp. 243-252.

Ganapathisubramani, B., Longmire, E. K. & Marusic, I., 2003, "Characteristics of vortex packets in turbulent boundary layers." *J. Fluid Mech.*, Vol 478, pp. 35–46.

Ganapathisubramani, B., Clemens, N. TT., & Dolling, D. S., 2006, "Large-scale motions in a supersonic turbulent boundary layer." *J. Fluid Mech.*, Vol 556, pp. 271–282.

Guala, M., Hommema, S. E., & Adrian, R. J., 2006, "Large-scale and very-large-scale motions in turbulent pipe flow." *J. Fluid Mech.*, Vol 554, pp. 521542.

Hutchins, N. & Marusic, I., 2007a, "Evidence of very long meandering structures in the logarithmic region of turbulent boundary layers". *J. Fluid Mech.*, Vol 579, pp. 1–28.

Hutchins, N. & Marusic, I., 2007b, "Large-scale influences in near-wall turbulence." *Phil. Trans. R. Soc. A*, Vol 365, pp. 647–664.

Mathis, R., Hutchins, N., & Marusic, I., 2009, "Large-scale amplitude modulation of the small-scale structures in turbulent boundary layers." *J. Fluid Mech.*, In Press.

Monty, J. P., Stewart, J. A., Williams, R. C., & Chong, M. S., 2007, "Large-scale features in turbulent pipe and channel flow." *J. Fluid Mech.*, Vol 589, pp. 147–156.

Tanahashi, M., Kang, S. J., Miyamoto, T. , Shiokawa, S. and Miyauchi, T., 2004, "Scaling law of fine scale eddies in turbulent channel flows up to $Re_\tau = 800$." *Int. J. Heat Fluid Flow*, Vol 25, pp. 331–340.

Tomkins, C. D. & Adrian, R. J., 2003, "Spanwise structure and scale growth in turbulent boundary layers." *J. Fluid Mech.*, Vol 490, pp. 37–74.

Wark, C. E., & Nagib, H. M., 1991, Experimental investigation of coherent structures in turbulent boundary layers.", *J. Fluid Mech.*, Vol 230, pp. 183–208.